ORIGINAL CONTRIBUTION

Rhinology, 48, 163-168, 2010

Impact of inferior turbinate hypertrophy on the aerodynamic pattern and physiological functions of the turbulent airflow - a CFD simulation model*

Xiao Bing Chen[1], Heow Pueh Lee[1], Vincent Fook Hin Chong[2], De Yun Wang[3]

[1] Department of Mechanical Engineering, Faculty of Engineering, National University of Singapore, Singapore
[2] Department of Diagnostic Radiology, Yong Loo Lin School of Medicine, National University of Singapore, Singapore
[3] Department of Otolaryngology, Yong Loo Lin School of Medicine. National University of Singapore, Singapore

SUMMARY

Introduction: *The aim of this study was to investigate the effects of nasal obstruction with enlargement of inferior turbinates on the aerodynamic flow pattern using Computational Fluid Dynamics (CFD) tools including the effects of turbulence.*

Methods: *A high-resolution 3-dimensional model of the nasal cavity was constructed from MRI scans of a healthy human subject using MIMICS 12.0 software. Nasal cavities corresponding to healthy, moderate and severe nasal obstructions were simulated by enlarging the inferior turbinate geometrically. Numerical simulations with turbulent flow models were implemented using FLUENTS for CFD simulations.*

Results: *In the healthy nose, the main respiratory air stream occurs mainly in the middle of the airway, accompanied by a diffused pattern of turbulent flow on the surface of the nasal mucosa. The peak value of turbulent flow is found in the functional nasal valve region. However, this aerodynamic flow pattern has partially or completely changed in the models with enlarged inferior turbinate. An inhalation flow rate of 34.8 L/min with a maximum velocity of 5.69 m/s, 7.39 m/s and 11.01 m/s are detected, respectively, in the healthy, moderately and severely obstructed noses. Both total negative pressure and maximum shear stress have increased by more than three and two times, respectively, in severely blocked noses compared to the healthy one.*

Conclusion: *Data of this study provide quantitative and quantitative information of the impact of inferior turbinate hypertrophy on the aerodynamic pattern and physiological functions of nasal airflow. By including the model of turbulent airflow, the results of this experimental study will be more meaningful and useful in predicting the aerodynamic effects of surgical correction of inferior turbinate hypertrophy.*

Key words: nasal cavity, nasal obstruction, computational fluid dynamics (CFD), turbulent airflow, shear stress, physiology

INTRODUCTION

The aerodynamics inside a human nasal cavity domain are complex due to its complicated internal geometry. The airflow patterns (laminar or turbulent) inside are mainly determined by two factors, namely nasal cavity morphology and flow rate. The generation of turbulence inside the nasal cavity can be due to the orientation of the nares, existences of the nasal sill, the nasal valve and the projected conchae [(1)]. Moreover, nasal obstruction can also significantly affect the nasal cavity morphology. It is one of the most common symptoms encountered in both primary care and in the Ear Nose & Throat (ENT) specialist clinics. In addition to anatomical malformation, inflammation of the nasal mucosa due to infection or allergy is the most common pathological cause of nasal obstruction that is commonly seen by edema and congestion of the nasal mucosa and inferior turbinates.

In a normal condition, inspiratory flow rate for an adult can range from 5 L/min to 12 L/min for calm breathing and increases to 40 L/min for abnormal conditions, such as exertion and physical exercise. An extreme flow rate can be as large as 150 L/min [(2)]. With such a range of flow rate, the

*Received for publication: May 27, 2009; accepted: September 22, 2009

DOI:10.4193/Rhin09.093

Reynolds number *(Re)* can range from 4×10^2 to 1.2×10^4. From the aspect of numerical simulation, turbulent flow happens when *Re* is larger than 2000 (30 L/min) inside a straight pipe. The onset of turbulence has been reported to occur at lower *Re* in complex geometries such as the respiratory tract compared with straight pipes [3]. Moreover, with nasal obstruction, the cross section along the nasal cavity is decreased, which may also increase the local flow intensity and greatly induce local turbulence. Thus it is reasonable and necessary to implement a turbulent flow model for the simulation for a large flow rate, e.g. 30 L/min inside the nose.

This study aims to investigate the effects of morphological variation (hypertrophy of inferior turbinate) on the aerodynamic flow pattern compared with a normal nose by using Computational Fluid Dynamics (CFD) tools including the effects of turbulence. CFD models enable detailed predictions of airflow patterns within the anatomically identical numerical models in a relatively shorter time. Such a method with turbulent models has been reported by many *in vitro* studies to predict the airflow patterns with respect to the effect of various anatomical factors on the patency of the nose. Examples include the study of general nasal turbulent flow pattern [4], aerosol deposition [5], obstruction sleep apnea [6], and nose sniffing [7] each using different turbulent models. However, the effect of inferior turbinate hypertrophy on the airflow pattern and its related nasal physiology with a turbulent model has not been well studied.

Based on our previous CFD study in nasal obstruction induced by inferior turbinate hypertrophy with laminar flow assumption [8], a turbulence model with a higher flow rate is added and the existence and distribution changes of turbulence with the two different severities of inferior turbinate expansion are investigated. The outcome on the functional performance or patency of the nose is examined and discussed.

MATERIALS AND METHODS

Model construction

The nasal airway geometry is constructed from MRI scans of a healthy human subject, who has been selected based on medical history, endoscopic nasal examination, and measurements of active rhinomanometry and acoustic rhinometry. The results of these assessments are within the normal range of our previous studies [9-11]. The scan images appear at an interval of 1.5mm along the vertical direction.

The segmentation was performed using Mimics version 12.0 (http://www.materialise.com/). The main passageway has been properly captured in the three dimensional model such as inferior, middle and superior turbinates, and nasopharynx.

3D computation

Thereafter a high-resolution 3D volume mesh comprising computational domain in the nasal cavity, as well as a surrounding air volume extending 10 cm outside the nostril, was constructed. A typical computational model would comprise about 2 million 3D tetrahedral grids and was generated by combination of several commercially available pre-processing software programs, including Mimics 12.0, Hypermesh 9.0 and TGrid 4.0. Besides that, an in-house code was also developed for the arbitrary shape modification to the inferior turbinate that would mimic various degrees of severity of nasal obstruction. The computational fluid dynamics simulations were performed using Fluents 6.3.22 (http://www.fluent.com/).

Computational fluid dynamic simulations

For the computational fluid dynamic simulations, the flow was assumed to be incompressible and quasi-steady. To account into the possible existences of turbulence, the Reynolds averaged Navier-Stokes equations were solved for the turbulence flow with a standard κ - ε model [12-14]. The turbulent intensity was set to be 6% and the dissipation rate was set at a dissipation length scale of 0.1 cm at the inlet and outlet boundaries.

A constant flow rate of 4.35, 8.7, 17.4, 34.8 or 52.2 L/min at the nasopharynx area was applied. At the external enclosure of the face, the pressure inlet boundary condition was applied with zero gauge pressure (atmospheric pressure).

MCA determination

The minimum cross sectional area (MCA) from the front end of nostril was found to be a cut plane located at 2.35 cm along the airflow direction. This location is compatible with the results obtained from acoustic rhinometric (A SRE 2100 acoustic rhinometer, Rhinometrics A/S, Lynge, Denmark) measurement from the same person prior to MRI examination. The method for turbinate expansion has been detailed in a previous paper [8]. It is performed in such a manner that the whole inferior turbinate is enlarged homogeneously outwards by about 1 mm and 2 mm for moderate and severe obstruction, respectively. These classifications can also be documented by approximately one-third reduction of the MCA (1.453 cm^2 in the healthy nose) for the moderate (0.873 cm^2) and two third (0.527 cm^2) for the severe obstruction. The ratio of MCA reduction in moderate and severe obstruction is similar to our previous study of nasal obstruction after nasal allergen challenge in patients with allergic rhinitis [11].

Table 1. Comparison of the flow properties for a healthy nasal cavity with different inhalation flow rates.

Flow rate (L/min)	Maximum velocity (m/s)	Maximum wall shear stress (pascal)	Volume average turbulence intensity	Volume average turbulence kinetic energy (m^2/s^2)
4.35	0.851	0.132	0.01%	$1.10\text{x } 10^{-5}$
8.7	1.53	0.301	0.10%	$9.0\text{x}10^{-3}$
17.4	3.17	0.520	1.08%	0.0271
34.8	5.69	1.48	7.11%	0.135
52.2	9.63	2.74	16.2%	1.56

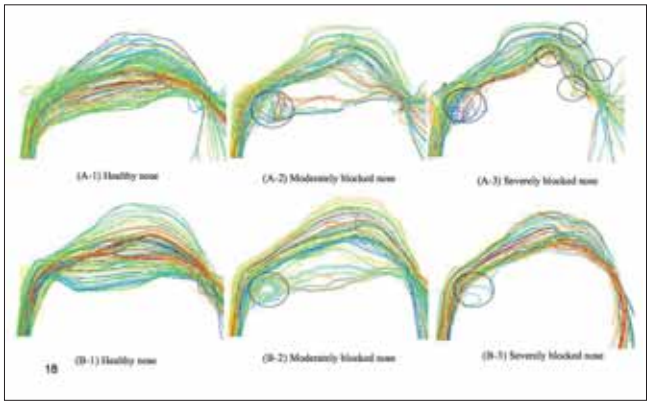

Figure 1. Inspiratory (A) and expiratory (B) nasal airflow (flow rate of 34.8 L/min) displayed in three types of nose mode. The vortex areas are circled.

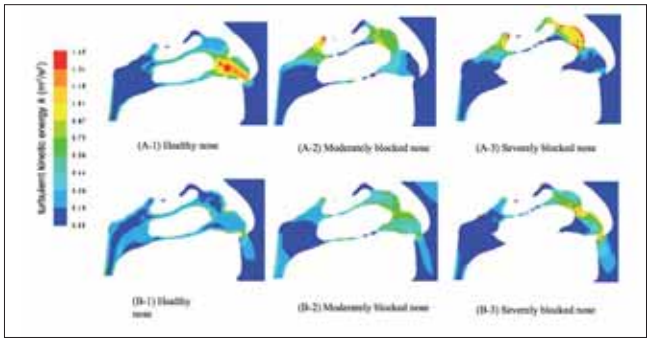

Figure 2. Contour of turbulent kinetic energy κ (m^2/s^2) with different degrees of patency at a coronal cross section during inspiration (A) and expiration (B). The flow rate implied is 34.8 L/min. Figure (A-1) has been published as a normal contour in Ref. 26.

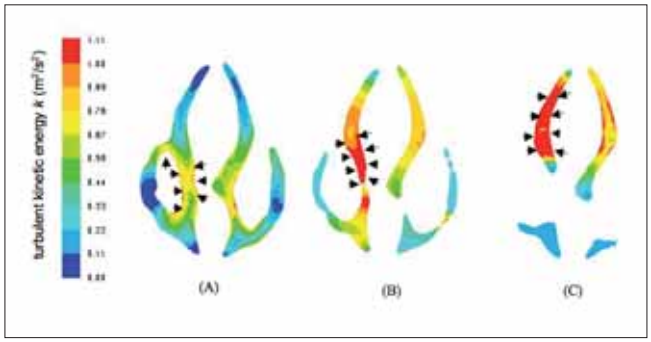

Figure 3. Contour of turbulent kinetic energy κ (m^2/s^2) with different degrees of patency at minimum cross section area during inspiration (with a flow rate of 34.8 L/min). (A) Healthy nose; (B) Moderately blocked nose; (C) Severely blocked nose. The arrows direct to the area with high levels of turbulence.

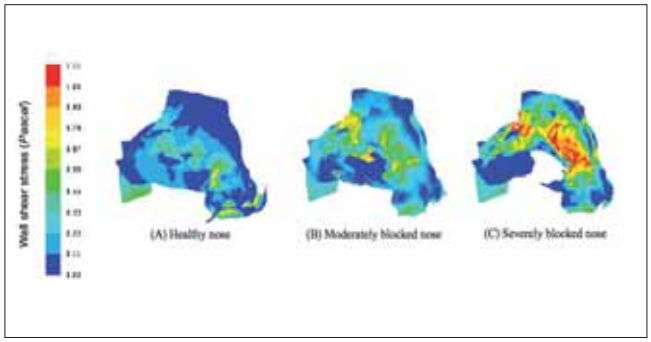

Figure 4. Wall shear stress *(Pascal)* of nasal cavity with different degrees of patency during inspiration. The flow rate is 34.8 L/min.

RESULTS

We first tested different flow rates of 4.35, 8.7, 17.4, 34.8 or 52.2 L/min (at the nasopharynx area) in the healthy nose model to configure a consistent flow rate that is able to generate turbulent flow in following experiments. It is noted that with a flow rate of 17.4 L/min (or smaller), there is low or no turbulent as the volume average turbulence intensity is 1.08% (Table 1). Therefore, a flow rate of 34.8 L/min has been chosen for all experiments in this study, as it allows a study of the changes of flow patterns in the nasal cavity more clearly with the presence and distributions of turbulent airflow.

Figure 1 shows the streamlines of both inspiratory (Figure 1A) and expiratory (Figure 1B) airflow that are found to occur mainly in the middle portion of the airway (between the inferior and middle turbinates and the septum). However, they (both in inspiration and expiration) have been redirected into the upper or superior part of the nasal airway in the moderately and severely blocked nose, due to the expansion (hypertrophy) of the inferior turbinate. Meanwhile, several vortex areas are detectable especially in the severely blocked nose (Figure 1).

Figure 2 shows the contour of turbulent kinetic energy for different degrees of patency at a coronal cross section with a consistent flow rate (34.8 L/min) during inspiration and expiration. It is noticeable that turbulent airflow is larger in intensity during inspiration than expiration in the healthy nose (Figures 2A-1 and 2B-1). The peak kinetic energy value of the turbulent airflow during inspiration is found to be in front of the anterior head of inferior turbinate, the area that is so called the functional nasal valve region [23,26]. However, this phenomenon does not exist anymore in both the moderately and severely blocked nose, probably due to the changes in aerodynamic pattern. Furthermore, in the healthy nose, turbulent airflow appears to be more prominent on the surface of the inferior turbinate mucosa and septum in the middle airway (Figure 3A). However, the intensity of turbulent airflow has increased and being moved upward into the upper or superior nasal cavity in the moderately (Figure 3B) or severely (Figure 3B) blocked nose. This phenomenon can be confirmed by distribution of the wall shear stress in the nasal cavity during inspiration (Figure 4).

To understand the relationship between airflow rates and intensity of turbulence under different conditions (a healthy,

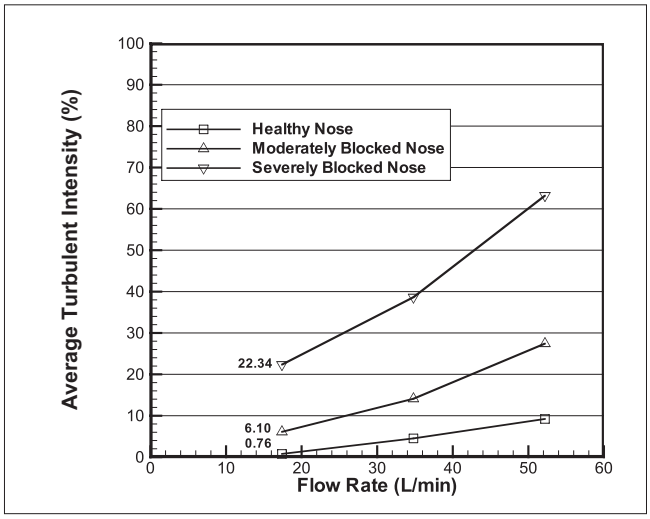

Figure 5. Average turbulent intensity (%) at minimum cross section area with different inspiration flow rates for different degrees of nasal patency.

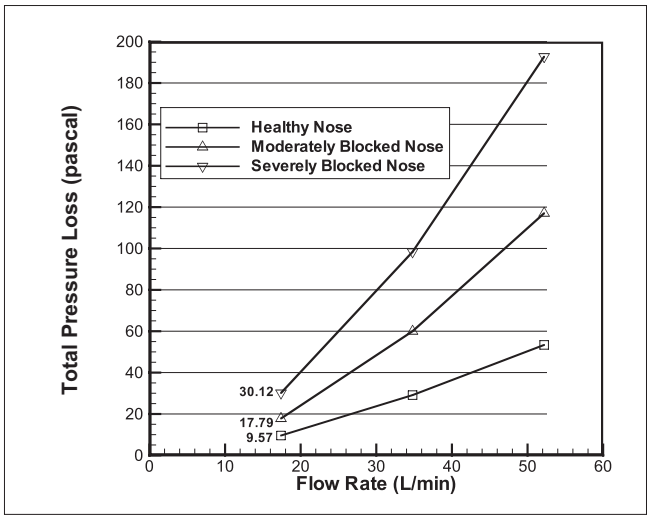

Figure 6. Total pressure loss (Pascal) with different inspiration flow rates for different degrees of nasal patency.

moderately and severely blocked nose) in the nasal cavity, a fixed area of MCA (2.35 mm from the nostril) has been chosen in all three models. Figure 5 shows the average (average mean surface) intensity of turbulent airflow differs obviously among the healthy (0.76%), moderately (6.10%) or severely (22.34%) blocked nose during inspiration (flow rate of 17.4 L/min), it increases proportionally when the flow rate is increased.

Figure 6 shows the total pressure loss (increase of negative pressure) in three conditions of nasal cavity with the changes of the intensity of inspiratory airflow rates. Total pressure is defined as the sum of dynamic pressure ($½\rho v^2$) and static pressure (ρ). So the total pressure loss is the difference of total pressure at the inlet and outlet, and can be described with the following formula:

$\Delta P_{total} = (½\rho v^2 + \rho)_{inlet} - (½\rho v^2 + \rho)_{outlet}$.

There was a much higher negative pressure in the moderately (17.79 ΔP) or severely (30.12 ΔP) blocked nose than in the healthy (9.57 ΔP) nose when there was a flow rate of 17.4 L/min. This difference increased proportionally when the flow rate increased.

DISCUSSION

Recently, we have reported the changes of airflow pattern in inferior turbinate hypertrophy using a computational fluid dynamics (CFD) model [8]. In that study, a laminar flow rate of 17.4 L/min was used in all CFD models. There may be criticism that the nasal airflow was not laminar and was a mixture of turbulent and orifice flow [19,21,22]. The existence of local turbulence in the nasal cavity is a controversial issue due to its complex geometry inside [1,5,7,15]. The wide range of flow rates from normal to abnormal breathing and the changes of turbinate morphology due to different physiological or pathophyiological conditions increase the degree of complexity for the flow patterns inside the nasal cavity. It has been reported experimentally that for a healthy nasal cavity with a flow rate smaller than 24 L/min, the flow inside is still laminar [16]. Thus it is reasonable and accurate enough to assume a laminar flow in a model when the flow rate is lowe than 20 L/min for numerical simulation [8].

Different from the previous paper (laminar flow assumption) [8], the current model focused on the existence and distribution changes of turbulence inside the nasal cavity with different severities of inferior turbinate expansion (Figure 2), which could affect the normal physiological functions, such as temperature and humidity distributions greatly [18]. Thus a larger flow rate than the one used in the previous paper [8] has been implemented to obtain better images of these results, although it may not be a normal breathing rate for the situation of rest. A similar distribution of turbulence and flow pattern were maintained with a smaller flow rate, however, the configurations and trends were less noticeable.

The existence of turbulence destabilizes the fluid boundary layer, which can maintain a steeper heat gradient or moisture transfer at the mucosal surface. Thus, heat and mass transfer can be enhanced and help particle deposition and removal of soluble gasses [7,12]. In the literature, however, there is neither quantitative nor qualitative data explaining the healthy status of a turbulent airflow as it can be largely influenced by the breathing pattern and internal structure of the nose, which is important for understanding of the physiological functions of the nose.

In this study, we are able to show some interesting characteristics of turbulent airflow.

1) In the healthy nose the average turbulent intensity is rather low during a calm breathing (Figure 5). However, it increased

rapidly, especially in a severely blocked nose (by almost 30-fold) at a fixed flow rate of 17.4 L/min. These differences can even be larger if the flow rate has increased in the moderately of severely blocked nose. It means that turbulent airflow occurs more frequently in subjects with nasal obstruction and/or during exertion and physical exercise.

2) The most intensive turbulent flow in the healthy nose is found in the functional nasal valve region that is a critical region for control of respiratory airflow [23]. However, it will not exit anymore in the presence of nasal obstruction due to inferior turbinate hypertrophy.

3) In the healthy nose, there is a diffused turbulent airflow with a moderate intensity on the surface (or boundary) of the inferior turbinate. It is known that the inferior turbinate has important physiological functions, as it constitutes a large area of respiratory mucosal with an extensive vascular bed in the nose. The presence of turbulent airflow will provide a better contact of the respiratory air with the functional airway mucosa, which is probably the most critical criterion for achieving the basic functions of the nose (e.g., air conditioning, heating, humidifying and clearing of the respiratory air). As the intensity and density of the turbulent flow increase in inferior turbinate hypertrophy, more studies are needed in order to understand the optimal range of the turbulent airflow, which is most favorable for achieving these functions.

Similar to our previous report, this study confirms an increased total negative pressure through out the nasal cavity during inspiration in moderately and severely obstructed nose, even during a calm breathing status [8]. It will increase even more rapidly when the flow rate is increased. Furthermore, an increased shear stress is also found, which is closely associated with the distribution and intensity of the turbulent airflow. However, it is still not fully understood how the qualitative and qualitative relationship is between the pattern and physical status of the respiratory air (e.g., flow rate, presence and location of turbulent airflow, pressure of the internal nasal cavity, wall shear stress), and all other known physiological functions of the nose.

Computational turbulent flow is much more of an art than laminar flow modeling [5,7,12,17,19,20]. It provides a more realistic and dynamic model for *in vitro* studies of the normality and relationship between morphological variations in the nasal cavity and their influence on respiratory airflow, which is somewhat difficult to be carry-out *in vivo* human studies. However, one shortcoming in this study is that the model of enlarging inferior turbinate was homogeneously and artificially throughout the entire turbinate on both sides. Such an artificial change of inferior turbinate was also previously implemented with a partial reduction [24] and complete removal on one side [18,25]. These papers reported a greatly disturbed intranasal airflow pattern and air-conditioning with sinus surgery, which helped to understand and interpret *in vivo* measured data. In the future, more histological and imaging studies are needed to have a realistic and statistical view of mucosa swelling in patients with inferior turbinate hypertrophy.

CONCLUSION

In conclusion, the presence of turbulent airflow is a crucial condition for achieving basic physiological functions of the nose. The location and strength of turbulent flow are very much influenced by the breathing pattern and anatomical conditions of the nasal cavity. Data of this numerical study provide qualitative and quantitative information of the impact of inferior turbinate hypertrophy on the airflow aerodynamic patterns, especially for the existence and distribution changes of turbulence inside the nasal cavity with different severities of inferior turbinate hypertrophy, which is difficult and relatively impossible to obtain from *in vivo* human studies. The nasal inspiration flow rate, presence and location of turbulent airflow, pressure of the internal nasal cavity, wall shear stress distribution can be influential for different physiological symptoms with realistic clinical scenarios (for example, breathing difficulty, local tissue blooding and sense of dryness or wetness). These data may be used in predicting the aerodynamic effects for the noses with inferior turbinate hypertrophy and give advisable hints on proper surgerical routes for correction in the future.

ACKNOWLEDGEMENT

The authors would like to acknowledge the financial support of the Academic Research Grant (T208A3103) from the Ministry of Education, Singapore. This project has been approved by the relevant Institutional Review Board.

CONFLICT OF INTEREST

The authors declare no conflict of interest.

REFERENCES

1. Churchill SE, Shackelford LL, Georgi JN, Black MT. Morphological variation and airflow dynamics in the human nose, Am J Human Biol. 2004; 16: 625-538.
2. Robert GH. Forced Inspiratory Nasal Flow - volume Curves, A Simple Test of Nasal Airflow. Mayo Clin Proc. 2001; 76: 990-994.
3. Chan TL, Schreck RM, Lippmann M. Effect of the laryngeal jet on particle deposition in the human trachea and upper bronchial airways. J Aerosol Sci. 1980; 11: 447-459.
4. Wen J, Inthavong K, Tian ZF, Tu JY, Xue CL, Li CG. Airflow Patterns in Both Sides of a Realistic Human Nasal Cavity for Laminar and Turbulent Conditions, 16th Australasian Fluid Mechanics Conference (AFMC); 2007: 68-74.
5. Liu Y, Matida EA, Gu JJ, Johnson MR. Numerical simulation of aerosol deposition in a 3-D human nasal cavity using RANS, RANS/EIM, and LES, J Aerosol Sci. 2007; 38: 683-700.
6. Jeong SJ, Kim WS, Sung SJ. Numerical investigation on the flow characteristics and aerodynamic force of the upper airway of patient with obstructive sleep apnea using computational fluid dynamics, Med Eng Phys. 2007; 29: 637-651.
7. Zhao K, Dalton P, Yang GC, Scherer PW. Numerical modeling of turbulent and laminar airflow and odorant transport during sniffing in the human and rat nose. Chem Senses. 2006; 31: 107-118.
8. Lee HP, Poh HJ, Chong FH, Wang DY. Changes of airflow pattern in inferior turbinate hypertrophy – a computational fluid dynamics model. Am J Rhinol. 2009; 23: 153-158.

9. Wang DY, Raza MT, Goh DYT, Lee BW, Chan YH. Acoustic Rhinometry in nasal allergen challenge study: which dimensional measures are meaningful. Clin Exp Allergy. 2004; 34: 1093-1098.
10. Huang ZL, Wang DY, Zhang PC, Yeoh KY. Evaluation of Nasal Cavity by Acoustic Rhinometry in the Ethnic Groups, Chinese, Malay and Indian. Acta Otolaryngologica (Stockh). 2001; 121: 844-848.
11. Huang ZL, Ong KL, Goh SY, Liew HL, Yeoh KH, Wang DY. Assessment of nasal cycle by Acoustic Rhinometry and Rhinomanometry. Otolaryngol Head Neck Surg 2003; 128: 510-516.
12. Inthavong K, Tian ZF, Li HF, et al. A numerical study of spray particle deposition in a human nasal cavity. Aerosol Sci Technol. 2006; 40: 1034-1045.
13. Fluent User's Guide, Release 6.3. Fluent Inc., October, 2006.
14. Piquet J. Turbulent flows: models and physics, Jean Piquet., Berlin, New York: Springer-Verlag, 1999.
15. Elad D, Liebenthal R, Wenig BL, Einav S. Analysis of Air Flow Patterns in the Human Nose. Med Biol Eng Comp. 1993, 31: 585-592.
16. Hahn I, Scherer PW, Mozell MM. Velocity profiles measured for airflow through a large-scale model of the human nasal cavity. J Appl Physiol 1993, 75: 2273-2287.
17. Shi H, Kleinstreuer C, Zhang Z. Laminar airflow and nanoparticle or vapor deposition in a human nasal cavity model. J Biomech Eng. 2006; 128: 697-706.
18. Lindemann J, Brambs HJ, Keck T, Wiesmiller KM, Rettinger G, Pless D. Numerical simulation of intranasal airflow after radical sinus surgery. Am J Otolaryngol. 2005; 26: 175-180.
19. Li W, Perzl M, Heyder J, et al. Aerodynamics and aerosol deaggregation phenomena in model oralpharyngeal cavities. J Aerosol Sci. 1996; 27: 1269-1286.
20. Katz IM, Davis BM, Martonen TB. A numerical study of particle motion within the human larynx and trachea. J Aerosol Sci. 1999; 30: 173-183.
21. Cole P. Acoustic rhinometry and rhinomanoemtry. Rhinology. 2000; Suppl 16: 29-34.
22. Kim JK, Yoon JH, Kim CH, Nam TW, Shim DB, Shin HA. Particle image velocimetry measurements for the study of nasal airflow. Acta Otolaryngol. 2006; 126: 282-287.
23. Eccles R. Nasal airflow in health and disease. Act Otolaryngol 2000; 120: 580-595.
24. Wexler D, Segal R, Kimbell J. Aerodynamic effects of inferior turbinate reduction: computational fluid dynamics simulation. Arch Otolaryngol Head Neck Surg. 2005; 131: 1102-1107.
25. Lindemann J, Keck T, Wiesmiller KM, Rettinger G, Brambs HJ, Pless D. Numerical simulation of intranasal airflow and temperature after resection of the turbinates. Rhinology. 2005; 43: 24-28.
26. Chen XB, Lee HP, Chong VFH, Wang DY. Assessment of Septal Deviation Effects on Nasal Air Flow-A Computational Fluid Dynamics Model. Laryngoscope. 2009; 119: 1730-1736.

De Yun Wang, MD, PhD,
Department of Otolaryngology
Yong Loo Lin School of Medicine
National University of Singapore
5 Lower Kent Ridge Road
Singapore 119260
Singapore

Tel: +65-6772 5373
Fax: +65-6775 3820
E-mail: entwdy@nus.edu.sg